Brain Endothelial Permeability Assay

Permeability assay was performed as described previously (Dohgu *et al.*, 2004). Briefly, MBEC4 cells were cultured on the collagen-coated polycarbonate membrane of a Transwell insert (Corning Coster Corp., MA). Before assay, the cells were washed with Krebs–Ringer buffer (118 mM NaCl, 4.7 mM KCl, 1.3 mM $CaCl_2$, 1.2 mM $MgCl_2$, 1.0 mM NaH_2PO_4, 25 mM $NaHCO_3$, 11 mM D-glucose, pH 7.4). Then, the buffer (1.5 mL) was added outside of the insert (abluminal side), and the buffer (0.5 mL) containing 100 μM of a chemical was loaded on the luminal side of the insert. Samples (0.5 mL) were recovered from the abluminal chamber at 10, 20, 30, and 60 min and replaced immediately with fresh Krebs–Ringer buffer. Sodium fluorescein (Na-F, MW 376; Sigma-Aldrich Corp., MO) was used as a paracellular transport marker, and chrysoidine (Tokyo Kasei Kogyo Co. Ltd., Tokyo, Japan) as a test chemical, in addition to quinacrine as a control. The chemical concentration was measured by either determining the fluorescent intensity of Na-F (Ex(λ) 485 nm; Em(λ) 530 nm) and quinacrine (Ex(λ) 450 nm; Em(λ) 530 nm) or determining the absorbance of chrysoidine at 450 nm. The permeability coefficient was calculated using the slope of clearance curve for each chemical obtained during the 60-min period according to the method described by Dehouck *et al.* (Dehouck *et al.*, 1992). Statistical analysis was performed using one-way analysis of variance followed by Tukey–Kramer method for multiple comparisons.

RESULTS

Antiprion Screening *in vitro*

To evaluate functional groups of antiprion chelating chemicals, various chelating chemicals were examined for whether they inhibited abnormal PrP formation in prion-infected ScNB cells. Thirty-five chelating chemicals were analyzed; 11 of them were effective in inhibiting abnormal PrP formation for doses at which cell toxicity was not observed (Tables I and II). Nine of the 11 effective chemicals had a common structure, which consisted of aromatic rings (terminals 1 and 2 in Table II) at both ends of an azo bond. Although both 4-methyl-2-(2-thiazolylazo)phenol and 4-(2-pyridylazo)resorcinol were not effective, they also exhibited this structure, with a thiazole ring and a pyridine ring in the terminal 1 portion, respectively. Their lack of effectiveness might be attributable to cell toxicity, which occurred at lower doses than for chemicals carrying a benzene ring in the terminal 1 portion. On the other hand, all chemicals carrying either a benzene ring or a naphthalene ring in the terminal 2 portion were effective. Therefore, the data suggest that a structure with such an aromatic ring as benzene or naphthalene in either end of an azo bond might be responsible for inhibiting abnormal PrP formation in ScNB cells.

Mechanism of Antiprion Action

We tested whether the effective chemicals cause any alteration of the cellular PrP level in the treated cells because reduction in the cellular PrP level engenders

Table I. Antiprion Activity in ScNB Cells of Chelating Compounds

Compound	IC_{50} (μM)	CM (μM)	Compound	IC_{50} (μM)	CM (μM)
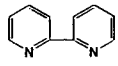	-	75	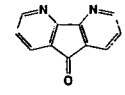	-	>100
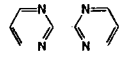	-	>100	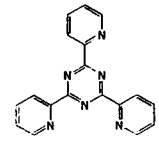	-	25
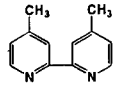	-	10	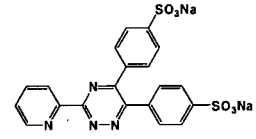	-	>100
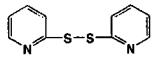	-	10	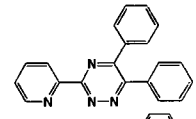	-	10
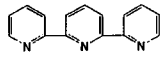	-	0.5	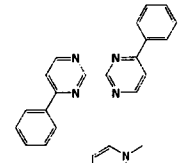	5	25
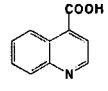	-	>100	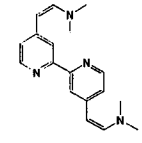	-	5
	-	5	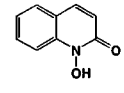	-	25
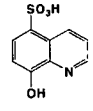	-	>100	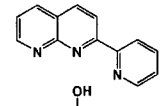	25	>200
	-	5	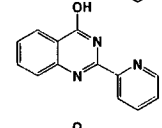	-	10
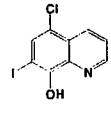	-	10	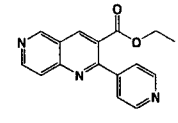	-	>100
			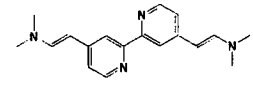	-	5

Note. IC_{50}: approximate dose giving 50% inhibition of abnormal PrP formation relative to the control. CM: approximate maximal dose that does not affect the rate of cell growth to confluence.

Table II. Antiprion Activity in ScNB Cells of Chelating Azo Compounds

Compound	Terminal 1 -N=N-	Terminal 2	IC_{50} (μM)	CM(μM)
Phenylazoresorcinol	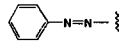	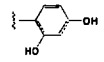	0.3	50
2-Phenylazo-4-methylphenol		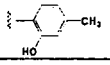	0.3	75
4-Methyl-2-(2-thiazolylazo)phenol	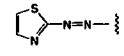	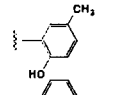	-	0.5
1-(2-Thiazolylazo)-2-naphtol		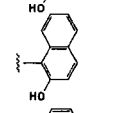	-	0.5
4-(2-Thiazolylazo)resorcinol		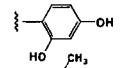	3	5
TAMSMB		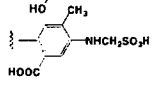	-	>100
4-(2-Pyridylazo)resorcinol	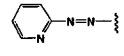	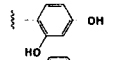	-	0.25
1-(2-Pyridylazo)-2-naphtol		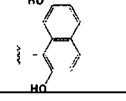	-	1
5-Br-PAPS	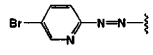	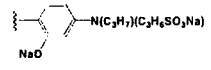	15	20
5-Br-PADAP		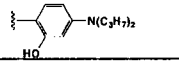	4	10
5-Cl-PADAP	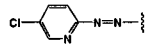	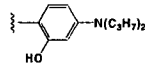	2	5
5-CF_3-PADAP	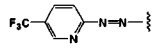	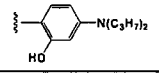	4	10
Yellow AB	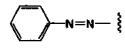	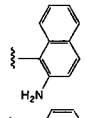	0.5	100
Chrysoidine		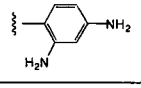	0.015	>100
Congo red	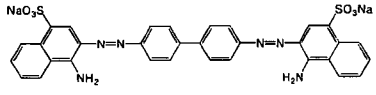		0.014	not tested
Quinacrine	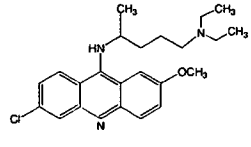		0.4	2

Note. IC_{50}: approximate dose giving 50% inhibition of abnormal PrP formation relative to the control. CM: approximate maximal dose that does not affect the rate of cell growth to confluence. TAMSMB: 4-methyl-5-sulfomethylamino-2-(2-thiazolylazo)benzoic acid. PAPS: 2-(2-pyridylazo)-5-[*N*-*n*-propyl-*N*-(3-sulfopropyl)amino]phenol, disodium salt. PADAP: 2-(2-pyridylazo)-5-diethylaminophenol.

reduction in abnormal PrP formation. The results revealed no reduction in the cellular PrP level of the cells (Fig. 1(A) and (B)). Furthermore, either to examine whether the chemicals directly destabilize or denature the abnormal PrP structure or to exclude the possibility of interference with preparation and immunodetection of the abnormal PrP, the cell lysate either alone or mixed with the chemicals was incubated at 37°C for 1 h prior to proteinase K digestion; it was then processed ordinarily to obtain the abnormal PrP. The results indicated that the chemicals did not affect the abnormal PrP signals (Fig. 1(C)).

Because it was predicted that the chemicals might exert their antiprion action through a certain mechanism involving chelating metals, the most effective chemical found here, chrysoidine, was preincubated before addition to the ScNB culture medium with an equivalent dose or lower doses of various metal ions, including copper, zinc, cobalt, and aluminum ions. The results revealed no change in the inhibition activity of the chemical (Fig. 2). Furthermore; to examine whether chelating activity is necessary for antiprion action, we modified Yellow AB in such a manner that its amino base was acetylated to remove its chelating activity. The acetylated Yellow AB was tested in ScNB cells, and it was one-eighth as effective in inhibiting abnormal PrP formation as Yellow AB (Fig. 3(A)). Finally, as a chemical bearing the effective structure but lacking chelating activity, the chemical azobenzene, which is most similar in the structure to the chemical chrysoidine, was tested. It was about 30 times less effective than chrysoidine (Fig. 3(B)). These findings suggest that chelating activity is not essential for the antiprion action but might influence it.

Interaction with Recombinant PrP

We previously reported that more potent antiprion agents have higher affinity to recombinant PrP121–231 in surface plasmon resonance (SPR) analysis (Kawatake *et al.*, 2006). Therefore, we examined whether this is also demonstrated in the effective chelating chemicals found here. Six of the chemicals (each at 50 μM) were tested. The SPR sensorgrams of the chemicals except 4-(2-pyridylazo)resorcinol showed similarly weak signal responses of less than 100 RU as quinacrine did (Fig. 4). However, neither 4-(2-thiazolylazo)resorcinol nor Yellow AB reached the equilibrium state at the association phase; neither 4-(2-thiazolylazo)resorcinol nor 2-phenylazo-4-methylphenol returned to the baseline at the dissociation phase. In contrast, 4-(2-pyridylazo)resorcinol showed the strongest response of more than 200 RU and neither reached the equilibrium state at the association phase nor returned to the baseline at the dissociation phase. The binding response value from the sensorgram (equilibrium or maximum response value divided by molecular weight), which is an index for estimating the interaction of a chemical with the molecules sited on a biosensor chip (Frostell-Karlsson *et al.*, 2000), showed no apparent relationship with the IC_{50} value of antiprion activity (data not shown), suggesting that the chemicals found here might exert their antiprion action in a manner that differs from those of previously reported antiprion chemicals such as antimalarias and amyloid binding dyes.

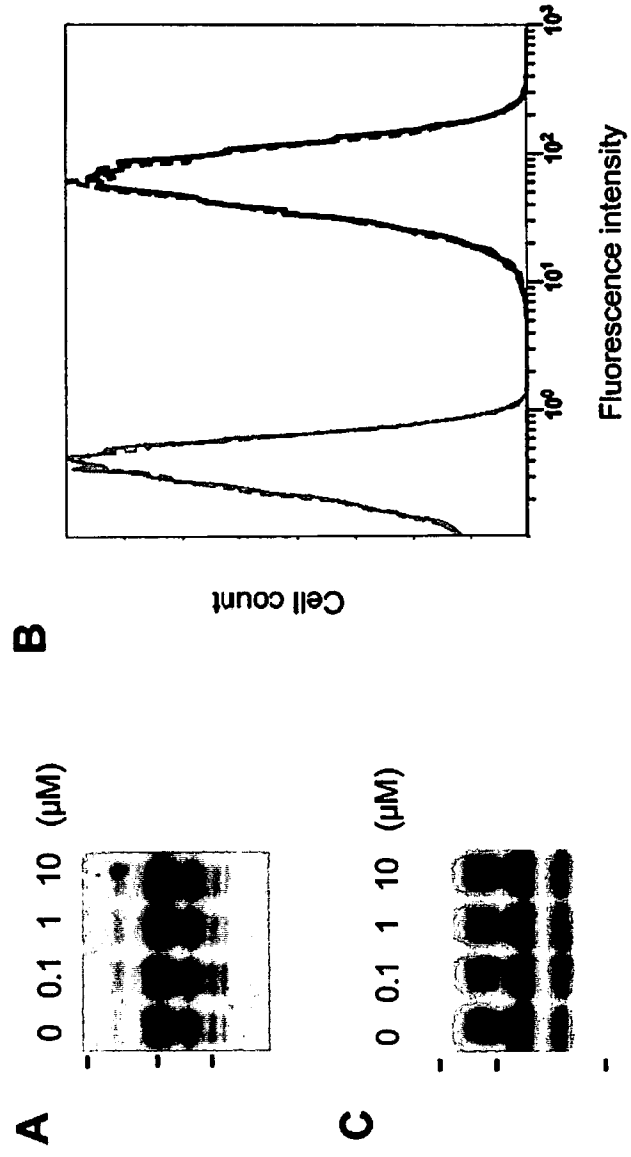

Fig. 1. Effects of a representative chemical, chrysoidine, on the cellular PrP (A, B) and the cell lysate abnormal PrP (C). (A) Immunoblot data of the total cellular PrP in noninfected NB cells treated with a designated dose of chrysoidine. *Bars* on the *left* indicate molecular size markers at 81, 42, and 32 kDa. (B) Flow cytometry data of the cell surface PrP in noninfected NB cells treated with 1 μM chrysoidine. *Solid line* and *broken line* indicate chrysoidine-treated cells and nontreated cells, respectively. *Grey line* peaks on the *left* show their respective isotype controls. (C) Immunoblot data of the abnormal PrP from ScNB cell lysate preincubated with a designated dose of chrysoidine prior to protease digestion. Molecular size markers on the left are 42, 32, and 18 kDa.

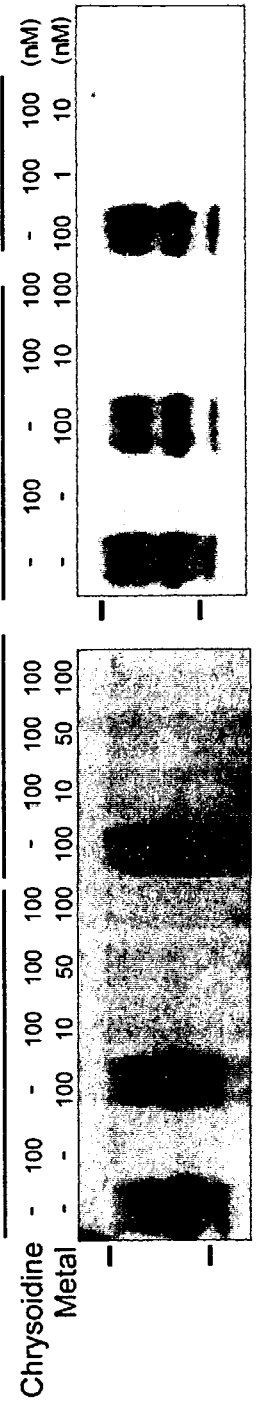

Fig. 2. Antiprion activity in ScNB cells of chrysoidine preincubated with metal ions. Immunoblot data of the abnormal PrP are shown. *Bars* on the *left* indicate molecular size markers at 37 and 25 kDa.

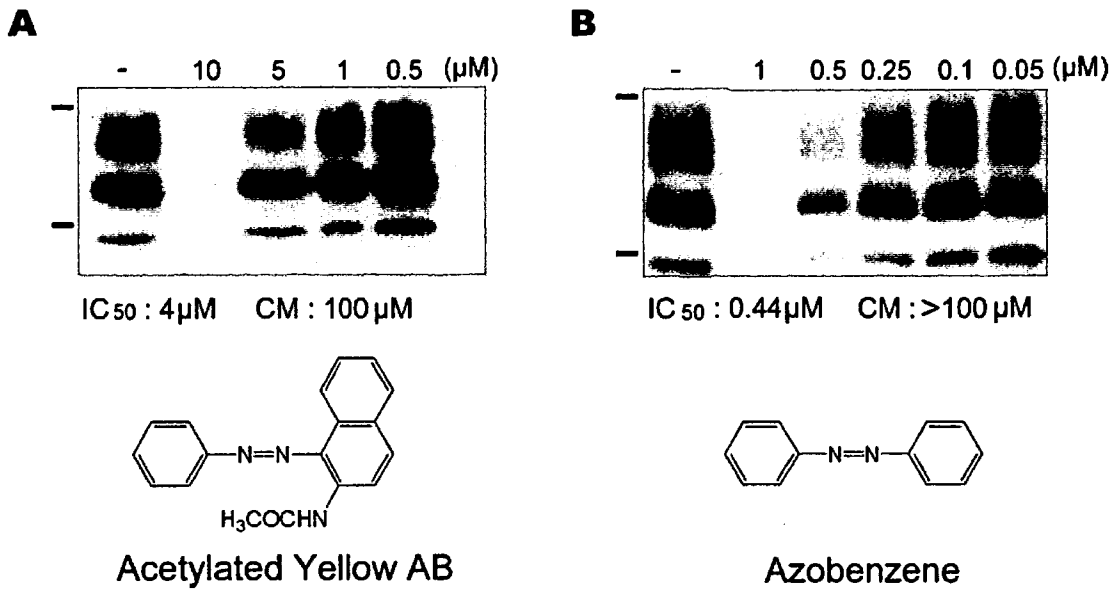

Fig. 3. Antiprion activity in ScNB cells of acetylated Yellow AB (A) and azobenzene (B) Immunoblot data of the abnormal PrP are shown. *Bars* on the *left* indicate molecular size markers at 37 and 25 kDa. IC_{50} is approximate dose giving 50% inhibition of abnormal PrP formation. CM is approximate maximal dose that does not affect the rate of cell growth.

Brain Endothelial Permeability

The brain is the main organ that is affected in prion diseases. Therefore, therapeutic compounds must penetrate into the brain. To examine the permeability of a chemical through the blood–brain barrier, we used a simple analytical model consisting of brain capillary endothelial MBEC4 cells. As a representative of the effective chemicals found in the study, chrysoidine was examined in this model and compared with a paracellular marker, Na-F, as well as a control, quinacrine, which has been used for clinical trials of patients with prion diseases. The results showed that the respective permeability coefficients of Na-F, quinacrine, and chrysoidine were 2.17×10^{-3}, 0.96×10^{-3}, and 4.63×10^{-3} cm/min (Fig. 5). Therefore, chrysoidine penetrated the brain capillary endothelial cells about five times more efficiently than quinacrine.

DISCUSSION

Here, we revealed that chelating chemicals, especially aromatic azo compounds, have antiprion activity. Mechanisms of their antiprion action apparently include neither alteration of cellular PrP level nor direct modification of abnormal PrP. Taken together with previous findings related to the interaction of PrP with metals (review in Brown, 2004), the data obtained through the present study suggest that the chelating activity might influence the antiprion action but is not essential for

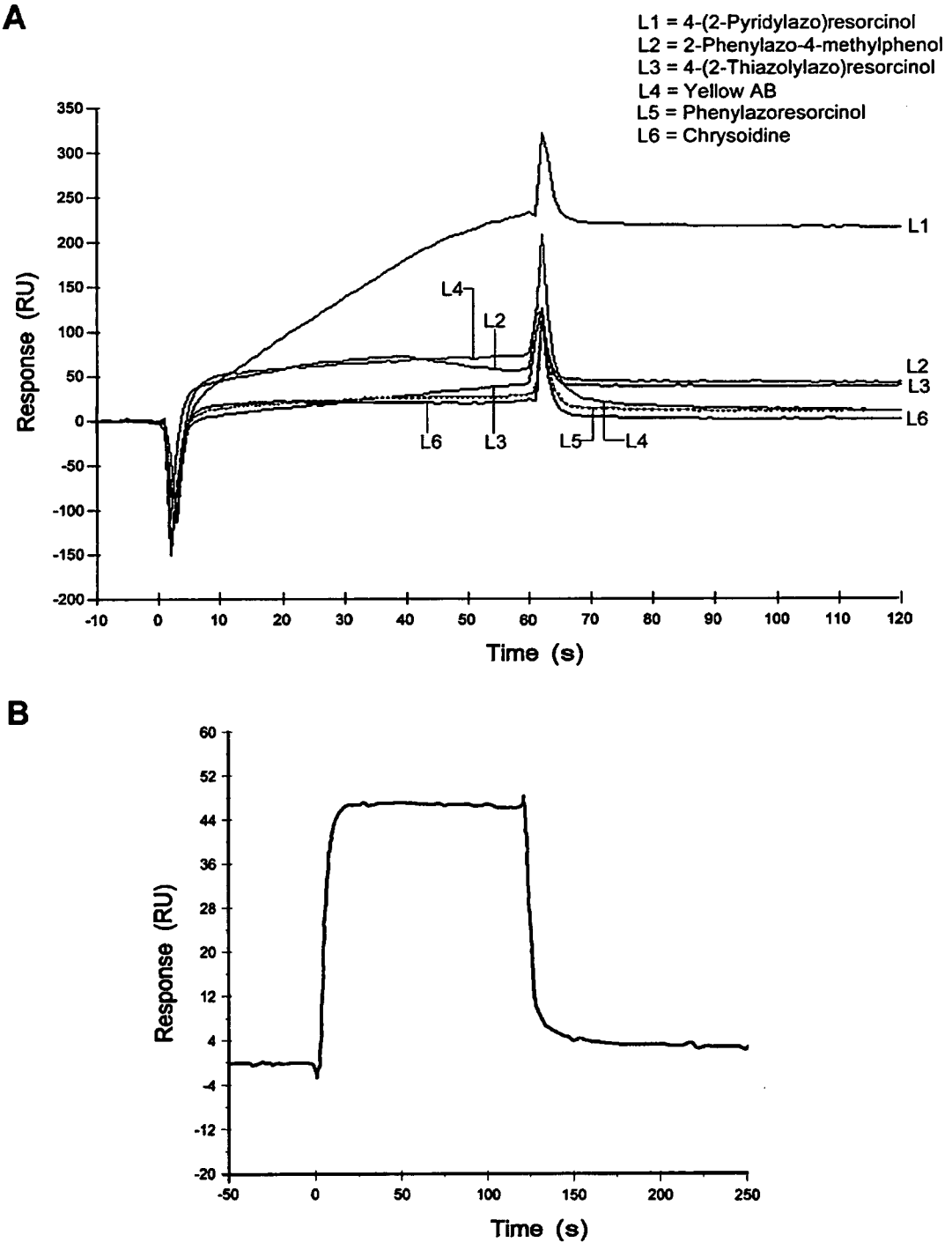

Fig. 4. SPR sensorgrams of chelating compounds (A) and quinacrine (B) interacting with PrP121–231.Each chemical at 50 μM was analyzed using a *ca.* 3,000 RU PrP-bound biosensor chip. Each phase of association and dissociation was monitored for 60 s in (A) or 125 s in (B).

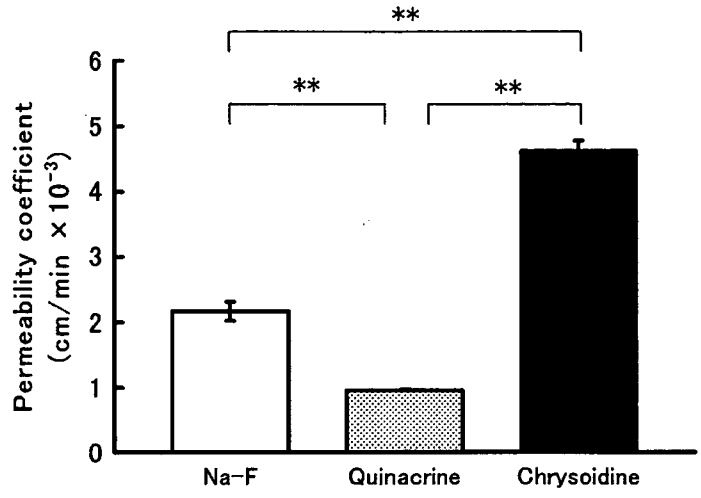

Fig. 5. Permeability coefficients of Na-F, quinacrine, and chrysoidine through MBEC4 monolayer. Each chemical at 100 μM was analyzed. The values are mean ± SEM (n = 3–4 inserts). $^{**}p < 0.01$; significant difference between each group.

it. This inference is consistent with our previous results from quinacrine derivatives carrying chelating activities (Murakami-Kubo *et al.*, 2004).

Chrysoidine, a representative chemical found in this study, is far superior to quinacrine in both the antiprion activity and the brain endothelial permeability. The respective antiprion activities of chrysoidine and quinacrine in ScNB cells were 15 nM and 400 nM in IC_{50}, indicating that chrysoidine is about 27 times more effective than quinacrine. Furthermore, chrysoidine penetrated brain capillary endothelial cells about five times more efficiently than quinacrine. In addition, chrysoidine is much less toxic than quinacrine because a maximal dose at which the ScNB cell growth to confluence is still tolerant was more than 100 μM in chrysoidine or 2 μM in quinacrine (Table II). These findings suggest that chrysoidine might be more beneficial *in vivo* than quinacrine, but the *in vivo* efficacy of chrysoidine remains to be evaluated.

Results from the SPR analysis obtained here were not consistent with those of our previous study (Kawatake *et al.*, 2006), where the SPR binding response correlates with the inhibition activity of abnormal PrP formation in ScNB cells. Chrysoidine, the most effective chemical in the study, has a similar structure to either half of a symmetrical compound, Congo red, whose antiprion activity (IC_{50} = 14 nM) is as prominent as that of chrysoidine (IC_{50} = 15 nM) (Table II) but whose permeability into the brain is reportedly very poor because of low lipophilicity and high charge in its acidic groups (Klunk *et al.*, 2002). Interaction with recombinant PrP121–231 differs greatly between chrysoidine and Congo red. Congo red has very high affinity (K_D = 1.6 μM) and strong binding response (1.7 RU/Da at 10 μM using a *ca.* 3,000 RU PrP-bound biosensor chip) to the PrP121–231 (Kawatake *et al.*, 2006), whereas chrysoidine shows a sensorgram pattern of low affinity compounds and has very low binding response (0.1 RU/Da at 50 μM using a similar

biosensor chip). These facts suggest that chrysoidine exerts its antiprion action in a manner that differs from that of Congo red, but this inference demands further evaluation.

The brain endothelial permeability assay using MBEC4 cells revealed that the permeability coefficient of quinacrine was much lower than that of Na-F. The results are consistent with those of our previous experiments (Dohgu *et al.*, 2004). Quinacrine transport through the blood–brain barrier is mediated by both the efflux system (P-glycoproteins) and the influx system (organic cation transporter-like machinery). Therefore, quinacrine entry into the brain is controlled by three factors: P-glycoprotein-mediated active efflux at the apical side of the plasma membrane; highly concentrative uptake system; large storage capacity in the cytoplasm of the brain endothelial cells. On the contrary, Na-F is transported through paracellular routes (tight junctions) at the blood–brain barrier, and neither active efflux nor concentrative uptake system is involved in the Na-F permeability. These differences might explain the reason why quinacrine is less efficiently permeabilized than Na-F.

Chrysoidine is used in various fields as a yellowish fluorescent dye. This chemical was suggested to relate with bladder cancer in humans (Cartwright *et al.*, 1983; Sole and Sorahan, 1985), but it is still controversial because the data of a later conducted case-control study denied its relation to the cancer (Sorahan and Sole, 1990). There are no data on the genetic and related effects of the chemical in humans, but it is mutagenic to bacteria and toxic to rat hepatocytes *in vitro* (Sandhu and Chipman, 1990). In the mice orally administered, it produced liver carcinoma, leukemia, and reticulum cell sarcomas (Anonymous, 1975). These findings suggest that clinical use of chrysoidine or related chemicals might be inadequate.

In conclusion, we screened chelating chemicals and found that chrysoidine was much more effective in both antiprion activity and brain endothelial permeability than quinacrine, and it was much less toxic in NB cells. The mechanism of antiprion action of this compound did not apparently include alteration of cellular PrP level, direct modification of abnormal PrP, or chelation of metals. Its interaction with PrP121–231 differed greatly from that of Congo red, despite their structural similarity. These findings will contribute to the development of therapeutic compounds for prion diseases.

ACKNOWLEDGMENTS

This study was supported by a Grant (H16-kokoro-024) to K.D. from the Ministry of Health, Labor, and Welfare, Japan. The authors thank Drs. Jiro Takata, Atsushi Yamauchi, Shinya Dohgu, Satoshi Kawatake, Toru Iwaki, and Kenta Teruya for their suggestions, and Ms. Kyomi Sasaki for manuscript preparation.

REFERENCES

Anomymous. (1975). Chrysoidine. *Int. Agency Res. Cancer Monogr.* **8**:91–96.
Brown, D. R. (2004). Metallic prions. *Biochem. Soc. Symp.* **71**:193–202.

Cartwright, R. A., Robinson, M. R. G., Glashan, R. W., Gray, B. K., Hamilton-Stewart, P., Cartwright, S. C., and Barnham-Hall, D. (1983). Does the use of stained maggots present a risk of bladder cancer to coarse fishermen? *Carcinogenesis* **4:**111–113.

Dehouck, M. P., Jolliet-Riant, P., Brée, F., Fruchart, J. C., Cecchelli, R., and Tillement, J. P. (1992). Drug transfer across the blood–brain barrier: Correlation between *in vitro* and *in vivo* models. *J. Neurochem.* **58:**1790–1797.

Dohgu, S., Yamauchi, A., Takata, F., Sawada, Y., Higuchi, S., Naito, M., Tsuruo, T., Shirabe, S., Niwa, M., Katamine, S., and Kataoka, Y. (2004). Uptake and efflux of quinacrine, a candidate for the treatment of prion diseases, at the blood–brain barrier. *Cell. Mol. Neurobiol.* **24:**205–217.

Doh-Ura, K., Iwaki, T., and Caughey, B. (2000). Lysosomotropic agents and cysteine protease inhibitors inhibit scrapie-associated prion protein accumulation. *J. Virol.* **74:**4894–4897.

Frostell-Karlsson, A., Remaeus, A., Roos, H., Andersson, K., Borg, P., Hamalainen, M., and Karlsson, R. (2000). Biosensor analysis of the interaction between immobilized human serum albumin and drug compounds for prediction of human serum albumin binding levels. *J. Med. Chem.* **43:**1986–1992.

Ishikawa, K., Doh-ura, K., Kudo, Y., Nishida, N., Murakami-Kubo, I., Ando, Y., Sawada, T., and Iwaki, T. (2004). Amyloid imaging probes are useful for detection of prion plaques and treatment of transmissible spongiform encephalopathies. *J. Gen. Virol.* **85:**1785–1790.

Kawatake, S., Nishimura, Y., Sakaguchi, S., Iwaki, T., and Doh-ura, K. (2006). Surface plasmon resonance analysis for the screening of anti-prion compounds. *Biol. Pharm. Bull.* **29:**927–932.

Kim, C.-L., Karino, A., Ishiguro, N., Shinagawa, M., Sato, M., and Horiuchi, M. (2004). Cell-surface retention of PrPC by anti-PrP antibody prevents protease-resistant PrP formation. *J. Gen. Virol.* **85:**3473–3482.

Klunk, W. E., Bacskai, B. J., Mathis, C. A., Kajdasz, S. T., McLellan, M. E., Frosch, M. P., Debnath, M. L., Holt, D. P., Wang, Y., and Hyman, B. T. (2002). Imaging Abeta plaques in living transgenic mice with multiphoton microscopy and methoxy-X04, a systemically administered Congo red derivative. *J. Neuropathol. Exp. Neurol.* **61:**797–805.

Murakami-Kubo, I., Doh-Ura, K., Ishikawa, K., Kawatake, S., Sasaki, K., Kira, J., Ohta, S., and Iwaki, T. (2004). Quinoline derivatives are therapeutic candidates for transmissible spongiform encephalopathies. *J. Virol.* **78:**1281–1288.

Nakajima, M., Yamada, T., Kusuhara, T., Furukawa, H., Takahashi, M., Yamauchi, A., and Kataoka, Y. (2004). Results of quinacrine administration to patients with Creutzfeldt–Jakob disease. *Dement. Geriatr. Cogn. Disord.* **17:**158–163.

Prusiner, S. B. (1991). Molecular biology of prion diseases. *Science* **252:**1515–1522.

Race, R. E., Caughey, B., Graham, K., Ernst, D., and Chesebro, B. (1988). Analyses of frequency of infection, specific infectivity, and prion protein biosynthesis in scrapie-infected neuroblastoma cell clones. *J. Virol.* **62:**2845–2849.

Sandhu, P., and Chipman, J. K. (1990). Bacterial mutagenesis and hepatocyte unscheduled DNA synthesis induced by chrysoidine azo-dye components. *Mutat. Res.* **240:**227–236.

Sole, G., and Sorahan, T. (1985). Coarse fishing and risk of urothelial cancer. *Lancet* **1:**1477–1479.

Sorahan, T., and Sole, G. (1990). Coarse fishing and urothelial cancer: A regional case-control study. *Br. J. Cancer* **62:**138–141.

Tatsuta, T., Naito, M., Oh-hara, T., Sugawara, I., and Tsuruo, T. (1992). Functional involvement of P-glycoprotein in blood–brain barrier. *J. Biol. Chem.* **267:**20383–20391.

ANTIMICROBIAL AGENTS AND CHEMOTHERAPY, June 2007, p. 2274–2277 Vol. 51, No. 6
0066-4804/07/$08.00+0 doi:10.1128/AAC.00917-06

Prophylactic Effect of Dietary Seaweed Fucoidan against Enteral Prion Infection[▽]

Katsumi Doh-ura,[1]* Tomoko Kuge,[2] Miyuki Uomoto,[1] Keiko Nishizawa,[1] Yuri Kawasaki,[1] and Masahiko Iha[3]

Department of Prion Research, Tohoku University Graduate School of Medicine, Sendai, Japan[1]; Department of Neuropathology, Graduate School of Medical Sciences, Kyushu University, Fukuoka, Japan[2]; and South Product Ltd., Okinawa, Japan[3]

Received 25 July 2006/Returned for modification 25 August 2006/Accepted 28 March 2007

Dietary seaweed fucoidan delays the onset of disease of enterally infected mice with scrapie when given orally for 6 days after infection, but not when given before the infection. This effect was not modified at a tested fucoidan dose range and appeared to reach the maximum level at a concentration of 2.5% or less in feed. Daily uptake of fucoidan might be prophylactic against prion diseases caused by ingestion of prion-contaminated materials, although further evaluation of its pharmacology remains to be done.

Transmissible spongiform encephalopathies, or prion diseases, are fatal neurodegenerative disorders that include Creutzfeldt-Jakob disease (CJD) and Gerstmann-Sträussler-Scheinker syndrome in humans and scrapie, bovine spongiform encephalopathy (BSE), and chronic wasting disease in animals. Recent outbreaks of BSE and variant CJD (vCJD), both of which are considered to occur through ingestion of BSE-contaminated materials (reviewed in reference 21), have necessitated the development of preventive measures against these diseases.

Sulfated polysaccharides, such as heparin, dextran sulfate, and pentosan polysulfate (PPS), are known either to prolong incubation periods in animals with prion diseases or to inhibit formation of pathogen-related abnormal prion protein (PrP) in prion-infected cells (reviewed in reference 3). Their therapeutic effects are attributed to inhibition of the conversion of normal PrP to abnormal PrP by either competitively binding to the normal PrP (4) or reducing normal PrP on the cell surface through stimulation of endocytosis (20). These large-molecule compounds are not taken up well from the gut to blood or from blood to the brain (a target organ of prion diseases). Therefore, these compounds are effective in cases of peripheral infection when given intraperitoneally, intravenously, or subcutaneously (8) and even in cases of intracranial infection when given intracerebroventricularly (5). Recently, PPS intracerebroventricular injection has been utilized for clinical trials of patients; the clinical outcome remains to be determined (17).

Fucoidans, complex sulfated fucosylated polysaccharides, are known to have various biological activities: anticoagulant, antiviral, antiparasital, anti-inflammatory, contraceptive, and so on, because of their ability to imitate patterns of sulfate substitution on glycosaminoglycans and other sulfated glycans (2). Some fucoidans are present in large quantities in dietary brown seaweed food products, which are eaten frequently in Asian countries (9). Here, we report that fucoidan from popularly eaten brown algae has antiprion activity and delays disease onset when it is ingested after the enteral prion infection.

Fucoidan was prepared from the brown seaweed *Cladosiphon okamuranus* Tokida (Fig. 1A) and subsequently tested as described previously (15). Briefly, the brown seaweed was suspended in distilled water adjusted to pH 3.0 with 30% HCl and heated at 100°C for 30 or 60 min. The suspension was centrifuged (10,000 × *g*) at room temperature, and the supernatant was filtered using Microza UF membrane (Asahi Kasei Chemicals, Japan). Then the retentate was washed with distilled water and lyophilized. The levels of fucose, uronic acid, and sulfate in the lyophilized preparation were determined by examining the results of the phenol-H_2SO_4 reaction and carbazole reaction and by ion chromatography, respectively. The purity and molecular mass of the lyophilized preparation were determined by gel filtration high-performance liquid chromatography. Two fucoidan preparations were used in the experiment: sample 1, with an average mass of 42.6 kDa and 87.8% fucoidan content; and sample 2, with an average mass of 140.4 kDa and 87.1% fucoidan content.

Inhibition of abnormal PrP synthesis in vitro was investigated as described previously (7, 12) in three different prion-infected neuroblastoma (NB) cells, each of which was persistently infected with a distinct prion strain from scrapie (RML or 22L) or human prion disease (Fukuoka-1). The cells were cultured for 3 days in the presence of fucoidan, and proteinase K-resistant abnormal PrP in the cell lysate was recovered by ultracentrifugation and analyzed by immunoblotting with three different anti-PrP antibodies, SAF83 against human PrP142-160 (SPI-BIO, France), PrP-2B against mouse/hamster PrP89-103 (5), and PrP-3B against mouse/hamster PrP218-232 (not published). The three antibodies produced the same immunoblot data in the following studies. Therefore, all immunoblot figures presented are of SAF83. The results from prion-infected NB cells showed that sample 2 of the higher-molecular-mass fucoidan more strongly inhibited abnormal PrP formation at half-maximum effective dosages ranging from 2.5 μg/ml to 5.0 μg/ml in all cells (Fig. 1B), suggesting that fucoidan exerts its antiprion activity in a prion strain-independent manner. The inhibition was irreversible, and even the most effective

* Corresponding author. Mailing address: Department of Prion Research, Tohoku University Graduate School of Medicine, 2-1 Seiryo-cho, Aoba-ku, Sendai, Miyagi 980-8575, Japan. Phone: 81-22-717-8232. Fax: 81-22-717-7656. E-mail: doh-ura@mail.tains.tohoku.ac.jp.

▽ Published ahead of print on 16 April 2007.

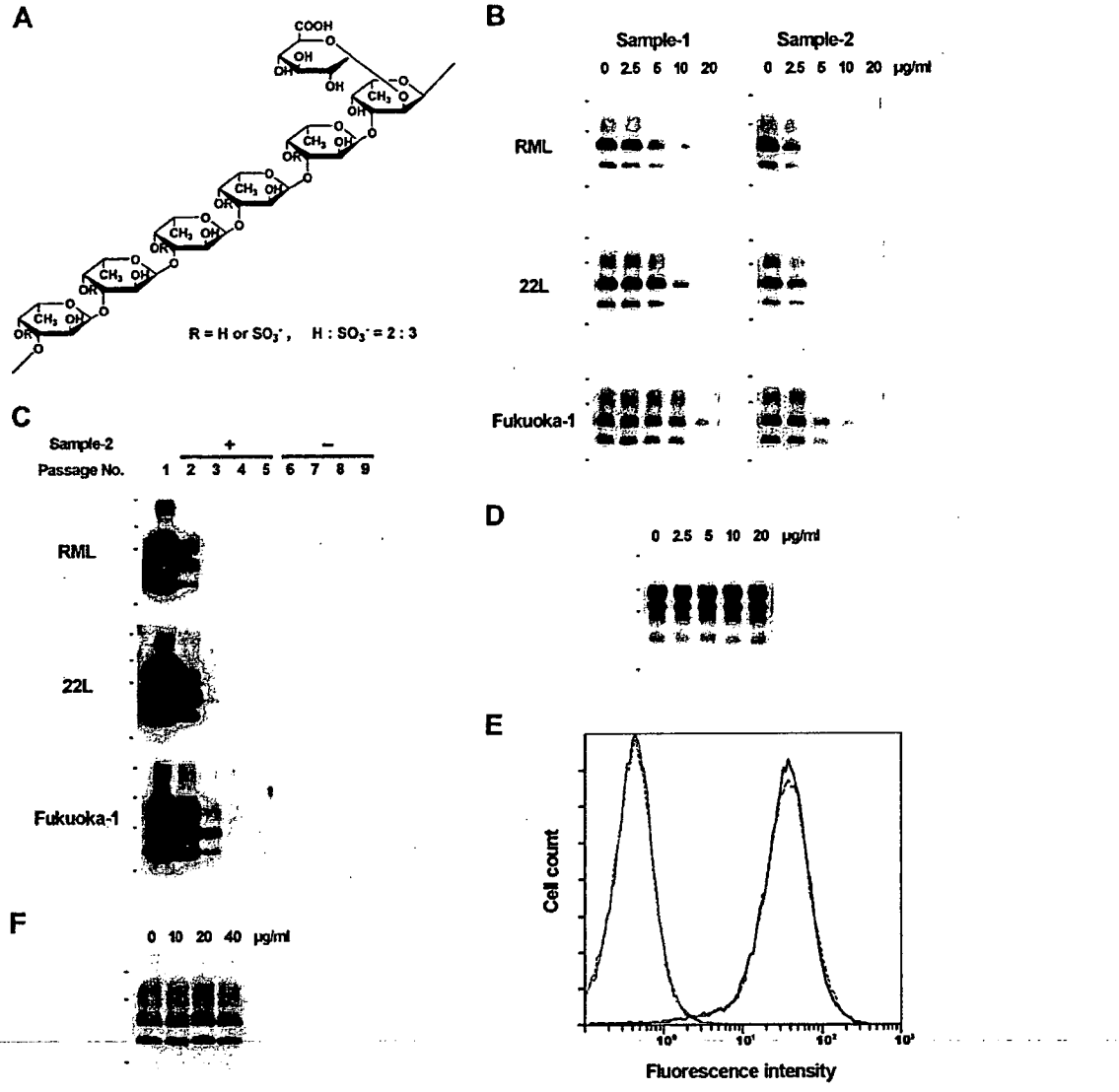

FIG. 1. Fucoidan and its effects on prion-infected or noninfected cells. (A) Chemical structure of fucoidan from *Cladosiphon okamuranus* Tokida. (B) Immunoblot analyses of abnormal PrP in the prion-infected NB cells treated with fucoidan. The small black bars to the left of the blots indicate the positions of molecular size markers at 42, 32, and 17 kDa. (C) Immunoblot analyses of abnormal PrP in the prion-infected NB cells serially passaged in the presence (+) and subsequently in the absence (−) of fucoidan. Overexposed images are shown. The small black bars to the left of the blots indicate the positions of molecular size markers at 81, 42, 32, and 17 kDa. (D) Immunoblot analysis of total normal PrP in noninfected NB cells treated with fucoidan. The molecular size markers to the left of the blot are the same as in panel C. (E) Flow cytometric analysis of normal PrP on the cell surface in noninfected NB cells treated with fucoidan. The solid line and broken line indicate fucoidan-treated cells and nontreated cells, respectively. Gray line peaks on the left show their respective isotype controls. (F) Immunoblot analysis of abnormal PrP from RML-infected cell lysate incubated with fucoidan prior to protease digestion. The molecular size markers to the left of the blot are the same as in panel B. All immunoblot data shown here are of SAF83.

abnormal PrP preparation technique, sodium phosphotungstic acid precipitation (18), never demonstrated that abnormal PrP signals that had once disappeared after treatment with 10 μg/ml of sample 2 fucoidan could reappear after serial passages in the absence of fucoidan (Fig. 1C). The inhibition mechanism included no alteration of either the total or cell surface level of normal PrP. That fact was demonstrated in noninfected NB cells treated with 20 μg/ml sample 2 fucoidan by either immunoblot analysis of the cell lysate without protease digestion or flow cytometric analysis performed as described previously (6) (Fig. 1D and E). In addition, apparent modification of the abnormal PrP with fucoidan was not observed in the immunoblot data when the RML-infected cell lysate was incubated with 20 μg/ml sample 2 fucoidan at 37°C for 1 h and processed to obtain the abnormal PrP as described (Fig. 1F). The findings are consistent with those of heparan sulfate mimetics (1, 19), but not those of PPS and dextran sulfate, which stimulate endocytosis of normal PrP on the cell surface and engender reduction of the total and cell surface normal PrP (20). Thus, reduction of normal PrP is not neces-

TABLE 1. Antiprion effects of fucoidan mixed with infectious inoculum

Expt no.	Fucoidan concn in inoculum (μg/ml)	Incubation period (days) (mean ± SD) (n^c)	Statistical significance
Expt 1[a]	200	57.9 ± 2.5 (8)	$P < 0.05^d$
	20	55.0 ± 2.5 (6)	
	2	54.2 ± 2.7 (5)	
	0.2	54.2 ± 3.9 (6)	
	0.02	53.7 ± 2.6 (6)	
	0 (control)	53.0 ± 2.7 (6)	
Expt 2[b]	200	73.3 ± 3.7 (7)	$P < 0.01^e$
	20	67.4 ± 7.2 (5)	
	2	69.0 ± 2.1 (5)	
	0.2	66.8 ± 4.6 (6)	
	0.02	64.4 ± 4.5 (7)	
	0 (control)	62.2 ± 2.2 (6)	

[a] Twenty microliters of 1% 263K prion homogenate mixed with the designated dose of sample 2 fucoidan was inoculated intracerebrally into each Tg7 mouse immediately after the mixture was made.
[b] Twenty microliters of 0.1% 263K prion homogenate with the designated dose of sample 2 fucoidan was inoculated intracerebrally into each Tg7 mouse after the mixture was incubated for 14 h at room temperature.
[c] Number of mice tested in each group.
[d] Statistical significance against the value for the control, analyzed using one-way analysis of variance followed by the Tukey-Kramer method for multiple comparisons.
[e] Statistical significance against the value for either the 0.02 μg/ml group or the control, analyzed as described in footnote *d*.

TABLE 2. Prophylactic effects of fucoidan feeding preinfection or postinfection

Time of feeding	Fucoidan concn in feed (%)	Incubation period (days) (mean ± SD) (n^c)	Statistical significance
Preinfection[a]	2.5	215.4 ± 40.5 (5)	
	5	243.4 ± 31.8 (5)	
	10	212.2 ± 37.7 (5)	
Postinfection[b]	2.5	346.8 ± 28.0 (5)	$P < 0.01^d$
	5	368.1 ± 73.9 (7)	$P < 0.01^d$
	10	367.4 ± 44.9 (5)	$P < 0.01^d$
Control		231.1 ± 28.3 (6)	

[a] Fucoidan feeding started 7 days prior to enteral inoculation by gavage feeding with 200 μl of 10% 263K prion homogenate and ended the day before inoculation.
[b] Fucoidan feeding started the day after enteral inoculation and continued for 6 days.
[c] Number of mice tested in each group.
[d] Statistical significance against either the value for the preinfection group or the control, analyzed as described in Table 1, footnote *d*.

sarily responsible for the antiprion action of sulfated polysaccharides.

In one antiprion in vivo test, prion homogenate was mixed with a test compound prior to intracerebral inoculation and injected into the animal brain to elucidate increased incubation times attributable either to inactivation of the inoculum or its presence in the brain at the time of infection. Sample 2 was more effective in vitro. Therefore, it was tested in this manner using an animal model comprising hamster scrapie prion strain 263K and Tg7 mice expressing hamster PrP (16). That model was chosen because it gives the shortest incubation times of all experimental animal models available and because antiprion activity of fucoidan was observed, irrespective of prion strains. In an initial experiment, immediately after 20 μl of 1% 263K prion homogenate equivalent to an infectivity titer of about 10^8 50% lethal dose (LD_{50})/g of tissue (5) was mixed with sample 2 fucoidan at its final concentration of 0 to 200 μg/ml, five to eight-week-old Tg7 mice per group were inoculated intracerebrally with the mixture. Only the mixture containing the largest amount of sample 2 significantly increased the incubation period ($P < 0.05$) compared to that of the control (experiment 1 in Table 1).

Next, to determine whether preincubation of the mixture enhances inactivation of the infectious inoculum, the prion homogenate-fucoidan mixtures, similarly prepared but containing 10 times more diluted homogenate, were incubated for 14 h at room temperature and then injected similarly into five to seven mice per group. Experiment 2 in Table 1 shows that only the mixture containing the largest amount of sample 2 significantly increased the incubation period ($P < 0.01$), as demonstrated similarly in experiment 1. The findings suggest that fucoidan itself does not modify infectivity of the inoculum, but its presence in the brain might inhibit prion replication or PrP conversion, probably in a manner similar to that observed in vitro. This inference is supported by results described in previous reports that PPS is effective in delaying the onset of disease of prion-infected animals when administered continuously into the brain (5) or even by bolus shots (13). However, there remains another possibility, the possibility that fucoidan can modify the infectivity in the inoculum very rapidly without a 14-h incubation.

Finally, the potential practical utility of fucoidan was investigated, especially its prophylactic effects against peroral and enteral prion infections such as those that occur in BSE and vCJD. Two different timings of fucoidan feeding, where fucoidan powder was given in a mixture with feed powder at three different levels (2.5, 5, or 10%) were designed to reveal its distinct effects in mice. In one, fucoidan feeding started 7 days prior to enteral inoculation into five to seven Tg7 mice per group by gavage feeding over a few hours with a total of 200 μl of 10% 263K prion homogenate (about 10^9 LD_{50}/g infectivity titer) and ended the day preceding inoculation to elucidate its preinfection prophylactic effects. In the other, fucoidan feeding started the day after the inoculation and continued for 6 days to elucidate its postinfection prophylactic effects. The results demonstrated that fucoidan feeding that commenced after the enteral inoculation delayed the disease onset for about half the time of the control incubation (Table 2). However, fucoidan feeding before the enteral inoculation did not affect the incubation time.

Low proportions of fucoidan are absorbed from the gut into blood (11) and excreted in urine (10), although little more is known of the detailed pharmacology of ingested fucoidan. Sulfated polysaccharides injected intraperitoneally or intravenously inhibit prion replication in the lymphoreticular system, which is involved in the delivery of prion from the gut to the brain (8, 14). Therefore, it can be speculated that fucoidan absorbed into blood exerts its effects by inhibiting prion replication in the lymphoreticular system. A gap of fucoidan effects between the preinfection and postinfection fucoidan feeding might be attributable to the rapid clearance of blood fucoidan

into urine when this is the case. Another possible mechanism of the postinfectious fucoidan effects might be that it facilitates the excretion of infectious materials from the gut. This inference is supported by the fact that seaweed polysaccharides and other natural polysaccharides alter the bacterial spectrum of the gut and assist detoxification (9). In contrast, fucoidan does not seem to act via a certain factor induced in the host because fucoidan administered until the day before inoculation was never effective.

There was no difference in prolonged incubation times among the three different fucoidan concentrations, although the feed consumption per mouse was not statistically different in each experimental group irrespective of the fucoidan level. This might occur because even the lowest concentration of fucoidan in feed surpasses its absorption threshold from the gut or because blood fucoidan concentrations are not parallel to ingested fucoidan doses. The latter was previously reported in humans, where only a threefold difference in blood plasma fucoidan concentrations was detected despite a 7.5-fold difference in ingested fucoidan doses (11). In addition, the stoichiometric relationship between blood fucoidan concentration and inhibitory activity against prion replication in vivo might also be attributable to the results observed here. However, these inferences remain to be elucidated.

The inoculum used in the study of enteral infection contained an extremely high titer of about 10^9 LD_{50}/g, although most of the inoculum might be excreted in feces, and presumably, a much lower titer may cause the infection. More satisfactory prophylactic effects by orally ingested fucoidan might be expected when prion infection in BSE or vCJD is presumed to occur through a lower level of infectivity than that used in this study. On the other hand, the data presented cannot exclude the possibility that the in vivo effects of fucoidan on the 263K prion strain are different from those on other strains. However, this did not occur during our previous experiments with a sulfated polysaccharide (5).

Finally, all fucoidan samples used here contained fucoidan at less than 90% of total weight. Therefore, it is possible that ingredients other than fucoidan exert the antiprion activity observed in this study. However, gel-filtrated samples, which contained 99.9% fucoidan with a mass of 100 to 190 kDa produced the same in vitro results (data not shown). Therefore, fucoidan itself of the dietary brown seaweed imparts the antiprion activity. Its daily ingestion has the potential to provide some prophylactic benefit against such oral or enteral prion infections as occurred in BSE and vCJD, but further studies must be done to elucidate the pharmacology of ingested fucoidan.

This work was supported by the Ministry of Health, Labor and Welfare (H16-kokoro-024) and the BSE Control Project of the Ministry of Agriculture, Forestry and Fisheries of Japan.

We thank Satoshi Kawatake for valuable suggestions and Kyomi Sasaki for manuscript preparation.

REFERENCES

1. **Adjou, K. T., S. Simoneau, N. Salès, F. Lamoury, D. Dormont, D. Papy-Garcia, D. Barritault, J. P. Deslys, and C. I. Lasmézas.** 2003. A novel generation of heparan sulfate mimetics for the treatment of prion diseases. J. Gen. Virol. 84:2595–2603.
2. **Berteau, O., and B. Mulloy.** 2003. Sulfated fucans, fresh perspectives: structures, functions, and biological properties of sulfated fucans and an overview of enzymes active toward this class of polysaccharide. Glycobiology 13:29R–40R.
3. **Cashman, N. R., and B. Caughey.** 2004. Prion diseases–close to effective therapy? Nat. Rev. Drug Discov. 3:874–884.
4. **Caughey, B., K. Brown, G. J. Raymond, G. E. Katzenstein, and W. Thresher.** 1994. Binding of the protease-sensitive form of PrP (prion protein) to sulfated glycosaminoglycan and Congo red. J. Virol. 22:163–167.
5. **Doh-ura, K., K. Ishikawa, I. Murakami-Kubo, K. Sasaki, S. Mohri, R. Race, and T. Iwaki.** 2004. Treatment of transmissible spongiform encephalopathy by intraventricular drug infusion in animal models. J. Virol. 78:4999–5006.
6. **Doh-ura, K., K. Tamura, Y. Karube, M. Naito, T. Tsuruo, and Y. Kataoka.** 19 January 2007. Chelating compound, chrysoidine, is more effective in both antiprion activity and brain endothelial permeability than quinacrine. Cell. Mol. Neurobiol. doi:10.1007/s10571-006-9122-0.
7. **Doh-Ura, K., T. Iwaki, and B. Caughey.** 2000. Lysosomotropic agents and cysteine protease inhibitors inhibit scrapie-associated prion protein accumulation. J. Virol. 74:4894–4897.
8. **Farquhar, C., A. Dickinson, and M. Bruce.** 1999. Prophylactic potential of pentosan polysulphate in transmissible spongiform encephalopathies. Lancet 353:117.
9. **Fitton, J. H.** 2003. Brown marine algae: a survey of therapeutic potentials. Altern. Complem. Ther. 9:29–33.
10. **Guimarães, M. A. M., and P. A. S. Mourão.** 1997. Urinary excretion of sulfated polysaccharides administered to Wistar rats suggests a renal permselectivity to these polymers based on molecular size. Biochim. Biophys. Acta 1335:161–172.
11. **Irhimeh, M. R., J. H. Fitton, R. M. Lowenthal, and P. Kongtawelert.** 2005. A quantitative method to detect fucoidan in human plasma using a novel antibody. Methods Find. Exp. Clin. Pharmacol. 27:705–710.
12. **Ishikawa, K., Y. Kudo, N. Nishida, T. Suemoto, T. Sawada, T. Iwaki, and K. Doh-ura.** 2006. Styrylbenzoazole derivatives for imaging of prion plaques and treatment of transmissible spongiform encephalopathies. J. Neurochem. 99:198–205.
13. **Kocisko, D. A., W. S. Caughey, R. E. Race, G. Roper, B. Caughey, and J. D. Morrey.** 2006. A porphyrin increases survival time of mice after intracerebral prion infection. Antimicrob. Agents Chemother. 50:759–761.
14. **Mabbott, N. A., and G. G. MacPherson.** 2006. Prions and their lethal journey to the brain. Nat. Rev. Microbiol. 4:201–211.
15. **Nagaoka, M., H. Shibata, I. Kimura-Takagi, S. Hashimoto, K. Kimura, T. Makino, R. Aiyama, S. Ueyama, and T. Yokokura.** 1999. Structural study of fucoidan from *Cladosiphon okamuranus Tokida*. Glycoconjugate J. 16:19–26.
16. **Race, R. E., S. A. Priola, R. A. Bessen, D. Ernst, J. Dockter, G. F. Rall, L. Mucke, B. Chesebro, and M. B. Oldstone.** 1995. Neuron-specific expression of a hamster prion protein minigene in transgenic mice induces susceptibility to hamster scrapie agent. Neuron 15:1183–1191.
17. **Rainov, N. G., I. R. Whittle, and K. Doh-ura.** 2005. Treatment options in patients with prion disease—the role of long term cerebroventricular infusion of pentosan polysulphate, p. 41–66. *In* T. Kitamoto (ed.), Prions—food and drug safety. Springer-Verlag, Tokyo, Japan.
18. **Safar, J., H. Wille, V. Itri, D. Groth, H. Serban, M. Torchia, F. E. Cohen, and S. B. Prusiner.** 1998. Eight prion strains have PrP^{Sc} molecules with different conformations. Nat. Med. 4:1157–1165.
19. **Schonberger, O., L. Horonchik, R. Gabizon, D. Papy-Garcia, D. Barritault, and A. Taraboulos.** 2003. Novel heparan mimetics potently inhibit the scrapie prion protein and its endocytosis. Biochem. Biophys. Res. Commun. 312:473–479.
20. **Shyng, S. L., S. Lehmann, K.L. Moulder, and D. A. Harris.** 1995. Sulfated glycans stimulate endocytosis of the cellular isoform of the prion protein, PrP^{C}, in cultured cells. J. Biol. Chem. 270:30221–30229.
21. **Taylor, D. M.** 2002. Current perspectives on bovine spongiform encephalopathy and variant Creutzfeldt-Jakob disease. Clin. Microbiol. Infect. 8:332–339.

JOURNAL OF VIROLOGY, Dec. 2007, p. 12889–12898 Vol. 81, No. 23
0022-538X/07/$08.00+0 doi:10.1128/JVI.01563-07

Orally Administered Amyloidophilic Compound Is Effective in Prolonging the Incubation Periods of Animals Cerebrally Infected with Prion Diseases in a Prion Strain-Dependent Manner▽

Yuri Kawasaki,[1] Keiichi Kawagoe,[2] Chun-jen Chen,[2] Kenta Teruya,[1] Yuji Sakasegawa,[1] and Katsumi Doh-ura[1]*

Department of Prion Research, Tohoku University Graduate School of Medicine, Sendai, Japan,[1] and Tokyo R & D Center, Daiichi Pharmaceutical Co., Ltd., Tokyo, Japan[2]

Received 18 July 2007/Accepted 4 September 2007

The establishment of effective therapeutic interventions for prion diseases is necessary. We report on a newly developed amyloidophilic compound that displays therapeutic efficacy when administered orally. This compound inhibited abnormal prion protein formation in prion-infected neuroblastoma cells in a prion strain-dependent manner: effectively for RML prion and marginally for 22L prion and Fukuoka-1 prion. When the highest dose (0.2% [wt/wt] in feed) was given orally to cerebrally RML prion-inoculated mice from inoculation until the terminal stage of disease, it extended the incubation periods by 2.3 times compared to the control. The compound exerted therapeutic efficacy in a prion strain-dependent manner such as that observed in the cell culture study: most effective for RML prion, less effective for 22L prion or Fukuoka-1 prion, and marginally effective for 263K prion. Its effectiveness depended on an earlier start of administration. The glycoform pattern of the abnormal prion protein in the treated mice was modified and showed predominance of the diglycosylated form, which resembled that of 263K prion, suggesting that diglycosylated forms of abnormal prion protein might be least sensitive or resistant to the compound. The mechanism of the prion strain-dependent effectiveness needs to be elucidated and managed. Nevertheless, the identification of an orally available amyloidophilic chemical encourages the pursuit of chemotherapy for prion diseases.

Transmissible spongiform encephalopathies, or prion diseases, are a group of fatal neurodegenerative disorders that include Creutzfeldt-Jakob disease (CJD) and Gerstmann-Sträussler-Scheinker syndrome (GSS) in humans and scrapie, bovine spongiform encephalopathy, and chronic wasting disease in animals. These disorders are characterized by accumulation in the brain of an abnormal isoform of prion protein (PrP), which is a main component of the pathogen, prion, or a pathogen itself and which is rich in beta-sheet structure and resistant to digestion with proteinase K (24). Recent outbreaks of variant CJD and iatrogenic CJD through use of cadaveric growth hormone or dura grafts in younger people have necessitated the development of suitable therapies.

Caughey and colleagues first found Congo red and sulfated glycans to inhibit abnormal PrP formation in vitro (5, 6), although Congo red was much earlier described as a staining device for prion amyloid rods (23). Since the discovery of the therapeutic activity of Congo red, amyloidophilic compounds such as amyloid dye derivatives and glucoseaminoglycan mimetics have been noted as one class of possible therapeutic candidates for prion diseases (4, 32). Recently, the most advanced progress with amyloidophilic compounds, which have an excellent ability to permeate through the blood-brain barrier, has been made in the field of diagnosis of Alzheimer's disease. Some amyloidophilic compounds are developed as imaging probes to visualize amyloid deposits in the brains of Alzheimer's disease patients using positron emission tomography or single-photon emission computed tomography technology (3). Some of these chemicals are also useful to visualize abnormal PrP amyloids of some types of prion diseases in the brain (2, 14, 15, 28, 30).

We previously reported that some of these amyloid-imaging probes are effective as antiprion compounds and prolong the incubation periods of animals cerebrally infected with prion disease (14). We also reported that a new class of amyloidophilic chemicals, styrylbenzoazole derivatives, which have better penetration through the blood-brain barrier and which show more discrete labeling of amyloid deposition in brain tissues affected by either Alzheimer's disease or prion diseases, are effective as antiprion chemicals (15, 19). However, the efficacy of these amyloidophilic compounds, intravenously administered weekly, was not remarkable but was rather limited. In addition, their effectiveness was suggested to be prion strain dependent, but this was not fully evaluated because of the limited availability of the compounds in quantity and dosing route. It can be assumed that elevated brain chemical levels are necessary for a compound's efficacy. Therefore, a multiple-dosing regimen, which causes more sustained elevation in brain chemical levels, might be preferable to a single weekly dosing. In this study, to ascertain undefined benefits and limitations of amyloidophilic compounds as therapeutic drug candidates for prion diseases, a new class of amyloidophilic compounds which have no similarity in chemical structure with previously reported antiprion compounds was synthesized and tested for either antiprion activity in vitro or therapeutic efficacy in vivo when administered orally as a mixture with feed.

* Corresponding author. Mailing address: Department of Prion Research, Tohoku University Graduate School of Medicine, 2-1 Seiryo-cho, Aoba-ku, Sendai, Miyagi 980-8575, Japan. Phone: 81-22-717-8232. Fax: 81-22-717-7656. E-mail: doh-ura@mail.tains.tohoku.ac.jp.

▽ Published ahead of print on 19 September 2007.

TABLE 1. Tested compounds and their inhibition of abnormal PrP formation in ScN2a cells

Compound	Chemical structure	Mol wt	Octanol-water distribution coefficient[a] (log $D_{6.8}$)	Inhibition of abnormal PrP (approximate EC_{50}, nM)[b]	Maximum tolerance dose[c] (μM)
cpd-B	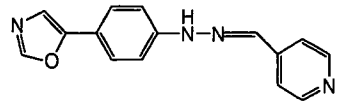	264	4.1	0.06	>10
cpd-D1	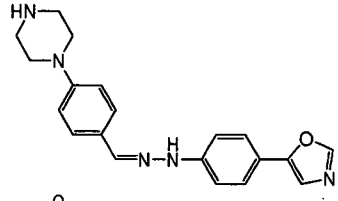	347	2.2	100	>10
cpd-D2	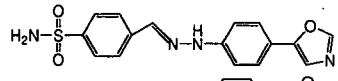	342	3.6	10	>10
cpd-D3	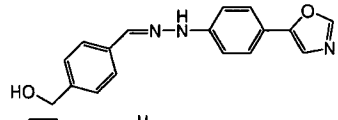	293	3.2	1	>10
cpd-D4	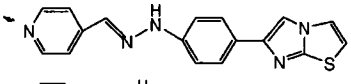	319	Not determined	1	>10
cpd-D5	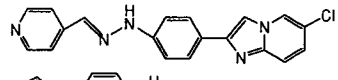	347	4.7	1	>10
cpd-D6	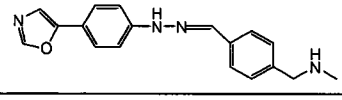	306	2.4	10	>10

[a] The distribution coefficient, a measure of a compound's hydrophilicity or hydrophobicity, was estimated using ChemAxon's calculator plugin software (Budapest, Hungary). The coefficients of medicines used for brain diseases are generally around 3.0.
[b] The approximate dose giving 50% inhibition of abnormal PrP formation relative to the control.
[c] The maximal dose that does not affect the rate of cell growth to confluence.

MATERIALS AND METHODS

Chemicals and experimental models. Test compounds were synthesized at the Tokyo R & D Center of Daiichi Pharmaceutical Co., Ltd. (Tokyo, Japan). The structures of the compounds are shown in Table 1. The compounds were dissolved in 100% dimethyl sulfoxide using ultrasonication and stored at −30°C until use.

Cultured cells were grown in Opti-MEM (Invitrogen Corp., Carlsbad, CA) supplemented with 10% fetal calf serum. As cellular models for the screening of antiprion compounds, either mouse neuroblastoma cells (N2a cells) or N2a cells with fivefold PrP overexpression (N2a-58 cells) which were persistently infected with a distinct prion strain were used, as follows: N2a cells infected with RML scrapie prion (ScN2a cells) (25), N2a cells with 22L scrapie prion (N167 cells), N2a-58 cells with RML scrapie prion (N002 or Ch2 cells), or N2a-58 cells with Fukuoka-1 GSS prion (F3 cells) (15). The Ch2 cells are a subclone of N002 cells.

Five-week-old Tga20 mice overexpressing murine PrP (11) or Tg7 mice overexpressing hamster PrP (26) were used as animal disease models after intracerebral infection with 20 μl of 1% (wt/vol) brain homogenate of RML prion, 22L prion, or Fukuoka-1 prion for Tga20 mice or 263K scrapie prion for Tg7 mice. Five-week-old ICR mice and Syrian hamsters were also used after they were infected intracerebrally with 20 μl of 1% (wt/vol) brain homogenate of RML prion or 40 μl of 1% (wt/vol) brain homogenate of 263K prion, respectively. Each animal was maintained under deep ether anesthesia for minimum distress during intracerebral inoculation. Permission for the animal study was obtained from the Animal Experiment Committee of Tohoku University, Japan.

In vitro PrP imaging. Autopsy-diagnosed brain samples from cases of GSS, which were kindly provided by Toru Iwaki from the Department of Neuropathology, Kyushu University, Japan, were used. After fixation in 10% buffered formalin for 2 weeks, the sample was immersed in 98% formic acid for reduction of prion infectivity, embedded in paraffin, and cut into 7-mm-thick sections. For neuropathological staining, deparaffinized sections were immersed in 1% Sudan black solution to quench tissue autofluorescence. They were then incubated for 30 min in 1 mM solution of compound B (cpd-B), rinsed with distilled water, and examined under a fluorescence microscope (DMRXA; Leica Microsystems GmbH, Wetzlar, Germany) using a fluorescein isothiocyanate filter set.

For comparison, each section was subsequently immunostained for PrP as described in a previous study (7). Briefly, the sections were treated with a hydrolytic autoclave and incubated with a rabbit primary antibody, anti-PrP-C, which was raised against a mouse PrP fragment consisting of amino acids 214 to 228 (1:200; Immuno-Biological Laboratories Co. Ltd., Gunma, Japan), followed by incubation with EnVision+System horseradish peroxidase labeling polymer (Dako, Glostrup, Denmark). The reaction product was developed with 3,3'-diaminobenzidine tetrahydrochloride solution and counterstained with hematoxylin.

In vitro treatment in cell cultures. Antiprion activity was evaluated by assaying the content of protease-resistant PrP (PrPres) in the cellular models, as described in earlier studies (6, 8, 18). Briefly, test compounds were added at the designated concentrations when cells were passaged at 10% confluence, while maintaining the final concentration of dimethyl sulfoxide in the medium at less than 0.5%. The cells were allowed to grow to confluence and were lysed with lysis buffer (0.5% sodium deoxycholate, 0.5% Nonidet P-40, phosphate-buffered saline [PBS]). For analysis of PrPres, samples were digested using 10 μg/ml proteinase K for 30 min at 37°C; the digestion was stopped using 1 mM phenylmethylsulfonyl fluoride. The samples were centrifuged at 100,000 × *g* for 30 min, and then pellets were resuspended in 1× sample loading buffer and boiled for 5 min. For analysis of the total level of cellular PrP in N2a cells treated with a test compound, cell lysates were mixed directly with one-quarter volume of 5× sample loading buffer and boiled for 5 min.

The samples were analyzed by immunoblotting. They were separated by electrophoresis on a 15% Tris-glycine–sodium dodecyl sulfate-polyacrylamide gel and electroblotted onto a polyvinylidene difluoride filter. The PrP was detected

using a monoclonal antibody, SAF83 (1:5000; SPI-Bio, Massy, France), followed by an alkaline phosphatase-conjugated goat anti-mouse antibody (1:20,000; Promega Corp., Madison, WI). Immunoreactivity was visualized using a CDP-Star detection reagent (Amersham, Piscataway, NJ). More than three independent assays were performed in each experiment.

The cell surface level of cellular PrP was assayed using flow cytometry, as described previously (10). Briefly, N2a cells dispersed by treatment with 0.1% collagenase (Wako Pure Chemical Industries Ltd., Osaka, Japan) were washed with ice-cold 0.5% fetal calf serum in PBS and incubated with SAF83 (1:500) or isotype-matched control immunoglobulin G1 for 20 min on ice. Cells were washed with 0.5% fetal calf serum in PBS and incubated with goat F(ab')2 fragment anti-mouse immunoglobulin G (heavy plus light chain)-phycoerythrin (1:100) (Beckman Coulter Inc., CA) for 20 min on ice. After washing, cells were analyzed using an EPICS XL-ADC flow cytometer (Beckman Coulter Inc., CA).

Pharmacokinetic studies. Brain cpd-B levels in the animals were assayed as described previously (20) after a 1-week feeding with 0.2% cpd-B ad libitum. All animals were sacrificed at 9:00 a.m. of day 8 by excision of the carotid artery under deep ether anesthesia to remove as much blood as possible, and the brain was collected, rinsed with saline, and weighed. Because preliminary studies found no significant difference in the data for perfused brains and nonperfused brains, the brain was not perfused with saline to remove residual blood. The brain was homogenized with 2 ml of 100% methanol for mouse brain or 4 ml for hamster brain. After centrifugation of the homogenate at 800 × *g* for 10 min, the supernatant was diluted with 9 volumes of 20 mM phosphate buffer, pH 6.5 (PB), and then filtered to obtain the sample for analysis. The sample was then applied to a conditioned C_{18} solid-phase extraction cartridge. The compound was eluted with methanol and was diluted with an equal volume of PB. The compound then was separated by high-performance liquid chromatography using a reversed-phase column (C_4, 4.6 × 150 mm; Phenomenex Inc., Torrance, CA). The compound was detected using a UV detector at 285 nm, and the dose of cpd-B per gram of brain tissue was determined.

The kinetics of brain uptake and washout of cpd-B were also investigated as described previously (20). The compound was solubilized in 5% Tween 80 in ethanol and then prepared as a 0.2-mg/ml solution containing 5% Tween 80 and 5% ethanol in saline. The compound at a dose of 1.0 mg/kg of body weight was administered intravenously to ICR mice under ether anesthesia. Both Tween 80 and ethanol are FDA-approved solubilizers of lipophilic medicinal chemicals. At the dose used in the study, neither solubilizer has been reported to cause any toxicity or to affect the pharmacokinetics. At 2 min or 30 min after injection, the blood was collected from the heart using heparin, and then the brain was obtained as described above. The blood plasma was mixed with 3 volumes of acetonitrile and centrifuged at 10,000 × *g* for 5 min. The supernatant was mixed with the same volume of PB and subsequently filtered to obtain the plasma sample for analysis. The preparation for the brain sample for analysis and the assay of the samples were performed as described above. The percentage of the injected dose per gram of tissue or fluid was used as a measure of the brain or plasma level of the compound.

In vivo treatment in animal models. In experimental animals that had been infected intracerebrally with a prion pathogen, cpd-B was given orally ad libitum as a mixture with powder feed at doses of 0.1%, 0.13%, 0.2%, and 0.33% by weight in the feed, corresponding, respectively, to ca. 150 mg/kg of body weight/day, ca. 225 mg/kg of body weight/day, ca. 300 mg/kg of body weight/day, and ca. 500 mg/kg of body weight/day in Tga20 mice, as each mouse consumed an average of 3.75 g of the feed per day. The animals were monitored every day until the terminal stage of disease; the incubation period, which was defined in the present study as the length of time from inoculation to the terminal stage of disease, was determined.

Pathological and infectivity assays. The right brain hemispheres of the mice were fixed using 10% buffered formalin and then embedded in paraffin. Three-micrometer-thick sections of the coronal slice sited at around one-third of the distance from the interaural line to the bregma line were dewaxed and immunostained using an anti-PrP-C antibody, as described above, or an antibody against glial fibrillary acidic protein (1:5,000; Dako, Glostrup, Denmark), as described in a previous study (9).

For detection of PrPres by immunoblotting, the left brain hemisphere was homogenized with 9 volumes of lysis buffer; after low-speed centrifugation, the supernatant was treated with 50 μg/ml proteinase K for 30 min at 37°C. An aliquot corresponding to 0.13 mg of brain tissue for PrPres assay or 0.83 μg of brain tissue for total PrP assay was electrophoresed on a 13.5% Tris-glycine–sodium dodecyl sulfate-polyacrylamide gel and analyzed by immunoblotting as described above.

For the infectivity assay, the left brain hemisphere was homogenized with PBS to produce a 10% brain homogenate. Serially diluted homogenate samples for assay were produced by diluting the brain homogenate serially with 10% brain homogenate of noninfected mice fed with 0.2% cpd-B for 1 month. A 20-μl aliquot of each sample was then inoculated intracerebrally into each of the Tga20 mice. Incubation times were assayed as described above.

Statistical analysis. Statistical significance was analyzed using the Kruskal-Wallis test followed by Scheffè's *F* test for multiple comparisons. Correlation analysis was performed using Spearman's rank correlation coefficient method. The regression coefficient was determined using simple linear regression analysis. The survival rate was calculated using the Kaplan-Meier method; its significance was evaluated using the log rank method.

RESULTS

Antiprion activity in vitro. The antiprion activities of newly synthesized compounds were investigated using ScN2a cells, which are N2a cells that are persistently infected with RML scrapie prion and are commonly used for drug screening. At a half-maximum effective concentration (EC_{50}) of about 60 pM, cpd-B inhibited PrPres formation (Table 1 and Fig. 1A). Other related compounds were also potent within a nontoxic dose range of up to 10 μM.

To investigate whether the efficacies of the compounds depend on the pathogen strain, cpd-B was tested in four other cell lines that had been infected individually with distinct prion strains. As shown in Fig. 1A, cpd-B was effective only in N002 (EC_{50}, 320 nM) and Ch2 (EC_{50}, 300 nM), both of which are N2a-58 cells infected with RML prion. However, the inhibitory activity in these cells was not as strong as that in ScN2a cells, which are derived from N2a cells expressing one-fifth of the normal PrP molecules of N2a-58 cells. In contrast, cpd-B was ineffective in both N167 cells (N2a cells infected with 22L scrapie prion) and F3 cells (N2a-58 cells infected with Fukuoka-1 GSS prion) at a dose of less than 10 μM. However, at a dose of 10 μM, a marginal reduction of the PrPres signals was observed in both cells. At a dose of greater than 10 μM, cell toxicity was observed. The results suggest that cpd-B exerts an inhibitory activity on PrPres formation in a prion strain-dependent manner: more effectively for RML prion and marginally for 22L prion or Fukuoka-1 prion.

The inhibition mechanism included no alteration of either the total or the cell surface level of normal PrP, as demonstrated in noninfected N2a cells treated with 1 μM cpd-B, using either immunoblot analysis of the cell lysate without protease digestion or flow cytometry analysis of the cell surface PrP (Fig. 1B and C). In addition, cpd-B did not facilitate the digestion of abnormal PrP by proteinase K, nor did it interfere with immunodetection, because PrPres signals were not modified after cpd-B was mixed and incubated with a cell lysate of nontreated ScN2a cells before proteinase K digestion (data not shown).

Pharmacological properties. Abnormal PrP amyloid imaging by cpd-B was performed on brain sections of GSS cases to examine the amyloidophilic properties of cpd-B. The compound bound to and fluorescently labeled most of the PrP plaques in cerebellar cortices of GSS cases (Fig. 1D). Background staining was barely observed after rinsing off the excess compound. Immunohistochemical analysis of PrP revealed that the compound achieved high-specificity labeling. The compound displayed no signal in control sections without amyloid lesions (data not shown).

Next, to examine the brain accessibility of cpd-B when administered orally, brain levels of cpd-B in the experimental

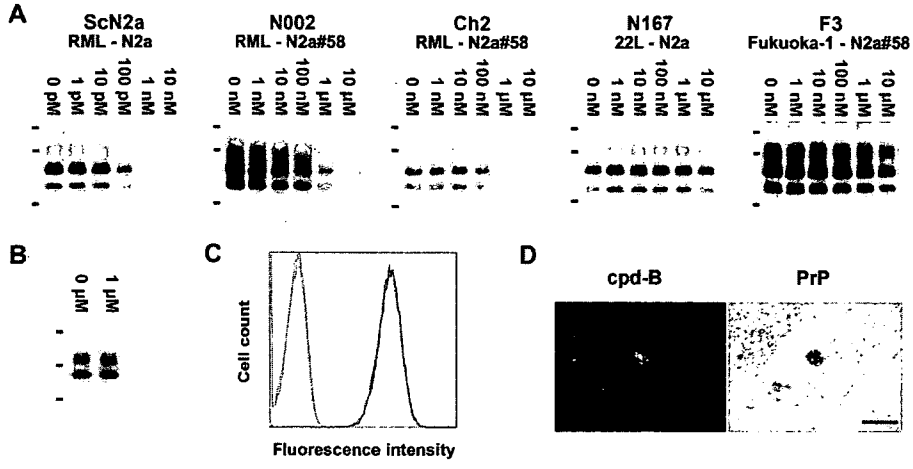

FIG. 1. cpd-B effects on prion-infected and noninfected cells and its amyloidophilic property. (A) Immunoblot analyses of PrPres formation in various prion-infected cells treated with the indicated concentrations of cpd-B. N2a-58 (N2a#58) is a stable transformant of N2a and expresses five-times-higher levels of PrP than N2a. Ch2 is a subclone of N002. The bars on the left are molecular size markers for 41, 32, and 18 kDa. (B) Immunoblot analysis of total normal PrP in noninfected N2a cells treated with cpd-B. Molecular size markers on the left are 47, 32, and 25 kDa. (C) Flow cytometric analysis of cell surface-normal PrP in noninfected N2a cells treated with 1 μM cpd-B. The solid and broken lines, respectively, indicate cpd-B-treated cells and nontreated cells. Gray line peaks on the left show their respective controls, using isotype immunoglobulin as a first antibody. (D) Imaging of abnormal PrP plaques in the brain tissue by cpd-B. Abnormal PrP deposition in a cerebellar tissue from a case of GSS was fluorescently labeled with cpd-B and subsequently immunostained with an anti-PrP antibody. Bar, 50 μm.

animals used in the study were assayed after the animals were fed ad libitum with 0.2% cpd-B-containing feed for 1 week. The brain level of cpd-B was 39.16 ± 22.15 nmol/g brain tissue in Tga20 mice (n = 4), 26.04 ± 12.50 nmol/g brain tissue in ICR mice (n = 4), and 22.94 ± 7.64 nmol/g brain tissue in Tg7 mice (n = 4). Syrian hamsters, however, showed a lower level, 7.26 ± 2.47 nmol/g brain tissue (n = 4). A considerable amount of cpd-B was detected in the brains of all experimental animals; no significant difference in the brain cpd-B levels was found among the types of the mice.

Further study of the pharmacokinetics of cpd-B in the blood and the brain was performed with ICR mice after cpd-B was injected into the tail vein. The percentage of the injected dose per gram of tissue or fluid was determined. The brain uptake level of cpd-B at 2 min after intravenous injection was 8.01% ± 1.27% of the injected dose/g tissue, whereas the blood plasma level was 2.92% ± 1.00%/g fluid. Consequently, the ratio of the cpd-B concentration in the brain to that in the blood plasma is 2.7:1, indicating that cpd-B is equal to the best brain-entering amyloidophilic chemicals previously identified (15). On the other hand, both the brain level and the blood plasma level of cpd-B at 30 min after the intravenous injection were below the measurable level of 50 pM, which indicates that cpd-B is very rapidly washed out from the brain and blood.

Regarding toxicity of cpd-B, body weight losses of about 16% in Tga20 mice and about 5% in Tg7 mice were observed after cpd-B was given orally ad libitum for 1 week at a dose of 0.33% weight in feed, which corresponds to ca. 500 mg/kg of body weight/day. Other doses of cpd-B tested in this study produced no apparent toxic effects in the experimental animals used.

Therapeutic efficacy in vivo. The therapeutic activity of cpd-B in vivo was assayed in murine PrP-overexpressing Tga20 mice that had been cerebrally infected with RML scrapie prion. The nontreated infected mice started exhibiting abnormal clinical signs such as staggering, rotating, irritation, and motionlessness at about 2 months after the infection; the mice then wasted into the terminal stage of disease in a week. Treatment by feeding cpd-B-containing feed ad libitum was initiated immediately after the infection and continued until the terminal stage of disease. The cpd-B-treated mice did not exhibit such abnormal signs as described above and wasted gradually into the terminal stage of disease. As shown in Fig. 2A, oral cpd-B treatment significantly prolonged the incubation periods of infected Tga20 mice in a dose-dependent manner; these were 68.5 ± 5.9 days in the nontreated control mice, 108.0 ± 2.8 days in the mice treated with 0.1% cpd-B feed, 120.5 ± 10.7 days in the mice with 0.13% cpd-B feed, and 154.3 ± 19.9 days in the mice with 0.2% cpd-B feed. Therefore, oral cpd-B treatment at the highest dose produced a 2.3-fold extension of the incubation periods of the mice. Statistical analyses demonstrated a significant linear correlation between the incubation periods and the cpd-B doses (r = 0.95; P < 0.01); the correlation equation was $y = 426.37x + 66.93$ (y, incubation period [days]; x, cpd-B dose [percentage in feed]), and the correlation coefficient was 0.89 (P < 0.01).

In our previous studies, the effectiveness of amyloidophilic chemicals in the extension of incubation periods of infected animals was observed only in Tga20 mice infected with RML prion (14, 15). ICR mice were then examined for the therapeutic efficacy of oral cpd-B treatment to investigate whether effectiveness of amyloidophilic compounds is restricted only to Tga20 mice. Nontreated control ICR mice that had been cerebrally infected with RML prion were in the terminal stage of disease at 154.2 ± 18.4 days postinfection, whereas the mice treated with 0.2% cpd-B feed lived significantly longer (P < 0.01). Even though the oral cpd-B treatment was discontinued at day 187 postinfection when the last of the nontreated animals reached the terminal stage of disease, more than half of the treated mice survived to day 270 postinfection (Fig. 2B).

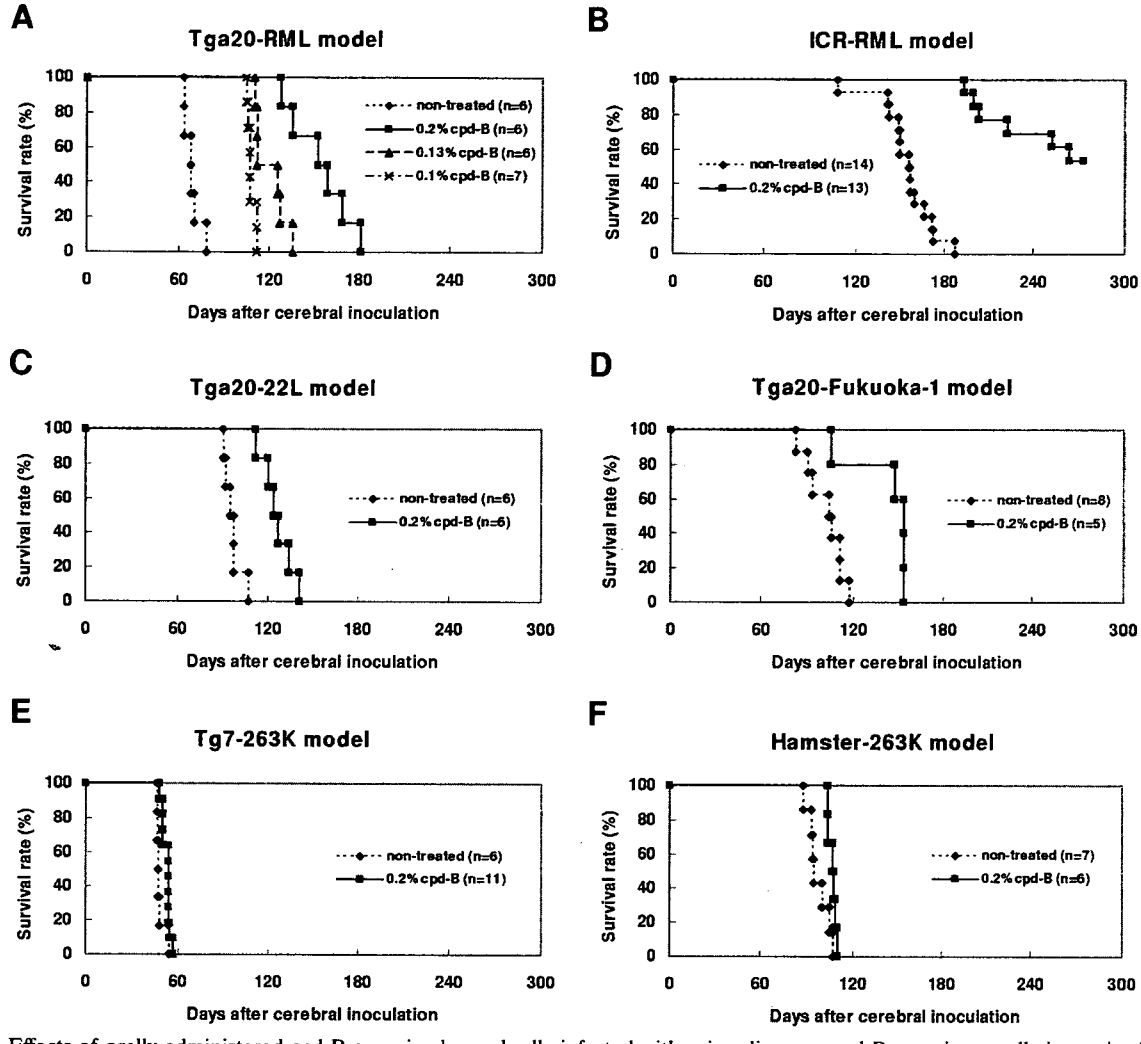

FIG. 2. Effects of orally administered cpd-B on animals cerebrally infected with prion diseases. cpd-B was given orally in a mixed form with powder feed ad libitum throughout the incubation periods in all animal disease models except the ICR-RML model, in which oral cdp-B treatment was discontinued at the time when the last of the nontreated animals reached the terminal stage of disease. In this study, the incubation periods are defined as the periods from the cerebral infection to the terminal stage of disease. Survival rates were calculated using the incubation periods and are plotted using the Kaplan-Meier method.

Next, the therapeutic efficacy of oral cpd-B treatment against other prion strains was investigated. The cpd-B treatment significantly prolonged the incubation periods of Tga20 mice that had been cerebrally infected with 22L scrapie prion ($P < 0.01$); these were 96.3 ± 5.9 days in the nontreated control mice and 126.3 ± 10.3 days in the mice treated with 0.2% cpd-B feed, indicating a 1.3-fold extension of the incubation period (Fig. 2C). Control mice started exhibiting distinguished opisthotonus with head rotating a week before the terminal stage of disease, whereas cpd-B treated mice showed no such clinical sign, even in the terminal stage.

cpd-B was also effective against Fukuoka-1 GSS prion. Cerebrally infected Tga20 mice lived significantly longer with oral cpd-B treatment ($P < 0.05$), i.e., 101.6 ± 12.1 days for the nontreated control mice and 142.2 ± 21.0 days for the mice treated with 0.2% cpd-B feed, indicating a 1.4-fold extension of the incubation period (Fig. 2D). Staggering was observed as an initial clinical sign in the control mice more than 1 week before the terminal stage of disease, although this clinical sign was not seen in the cpd-B treated mice.

In contrast to the case for these prion strains, the efficacy of oral cpd-B treatment was very marginal for 263K scrapie prion when Tg7 mice expressing hamster PrP were used as the host (Fig. 2E). The incubation periods of the cpd-B-treated mice (52.7 ± 2.8 days) were significantly but very marginally longer than those of the nontreated mice (48.0 ± 3.0 days) ($P < 0.05$). This prion is a hamster-adapted scrapie prion strain; Syrian hamsters were used as the host to examine whether the marginal efficacy of oral cpd-B treatment is attributable chiefly to the host Tg7 mouse or to the pathogen strain 263K prion. As observed in Tg7 mice, hamsters treated with 0.2% cpd-B feed also exhibited a marginal increase in the incubation period compared to that of the nontreated control hamsters that had been cerebrally infected with 263K prion ($P < 0.05$): 107.0 ± 2.5 days in the cpd-B treated hamsters and 97.4 ± 6.9 days in the non-